CLEANER
Clean Heat and Power from Hydrogen

CLEAN HEAT AND POWER FROM HYDROGEN

Grant agreement no.: 101137799
Start date: 01.01.2024 – **Duration**: 48 months.
Project Coordinator: Anders Ødegård, SINTEF

DELIVERABLE REPORT

D3.1: STABLE N-HTC CARBON SUPPORTS		
Due Date	31.12.2024 (extended to 30.06.2025)	
Author (s)	Julian Martin, Julian Mitrovic, Prof. Dr. Anna Fischer (UFR)	
Workpackage	3	
Workpackage Leader	UFR	
Lead Beneficiary	UFR	
Date released by WP leader	30.06.2025	
Date released by Coordinator	30.06.2025	
DISSEMINATION LEVEL		
PU	*Public*	✗
SEN	*Sensitive, limited under the conditions of the Grant Agreement;*	
NATURE OF THE DELIVERABLE		
R	*Document, report*	✗
DEM	*Prototype demonstrator*	
DEC	*Website*	
DMP	*Data management plan*	
OTHER	*Software, algorithms, models*	

SUMMARY	
Keywords	*Hydrothermal carbon, Upscaling, Enhanced Corrosion Stability, Catalyst carbon support*
Abstract	*This work presents the successful scale-up of the synthesis of nitrogen-doped hydrothermal carbon (N-HTC) supports to larger batch sizes, ensuring adequate material supply for further applications, such as catalyst design envisioned in the CLEANER project. Optimization of the graphitization degree by high temperature treatments results in improved resistance to electrochemical carbon corrosion. Moreover, the use of a ^{13}C-labeled carbon precursor enables the fabrication of fully ^{13}C-labeled N-HTC supports, providing a novel diagnostic tool for investigating electrochemical carbon corrosion mechanisms occurring in PEMFCs in detail.*

REVISIONS			
Version	**Date**	**Changed by**	**Comments**
0.1	05.12.2024	Julian Martin	1st draft; not all experimental data implemented
1.0	04.06.2025	Julian Martin	Experimental data implemented
1.1	16.06.2025	Anna Fischer / Julian Martin	Reviewed by UFR; sent to partners
1.2	30.06.2025	Minor text edits	Final

The CLEANER project is supported by the Clean Hydrogen Partnership and its members. The project is co-funded by the Research Council of Norway and the UK Research and Innovation (UKRI) under the UK government's Horizon Europe funding guarantee.

Co-funded by the European Union. Views and opinions expressed are however those of the author(s) only and do not necessarily reflect those of the European Union or Clean Hydrogen JU. Neither the European Union nor the granting authority can be held responsible for them..

STABLE N-HTC CARBON SUPPORTS

CONTENTS

1. Introduction 4
1.1 Context and Relevance 4
1.2 Objectives 5
2. Material and Methods 6
2.1 Chemicals and equipment 6
2.2 General hydrothermal synthesis 6
2.3 Characterization methods 7
3. Development of hydrothermal carbon supports 10
3.1 Synthesis of Nitrogen-doped hydrothermal carbon supports (N-HTC) in small scale 10
3.2 Synthesis of Nitrogen-doped hydrothermal carbon supports (N-HTC) in large scale 12
3.3 Tuning of graphitization degree 14
3.4 Synthesis of high surface area (HSA) carbon supports 15
3.5 Cost reduction via the use of lower grade precursors 17
3.6 Implementation of ^{13}C labeling 18
4. Carbon corrosion 21
4.1 Enhancing stability via graphitization of N-HTC materials 21
4.2 Implementation of ^{13}C labeling 22
5. Summary of work and conclusions 24
6. Bibliography 26
7. Appendix 28
7.1 Appendix A. 28

1. INTRODUCTION

In the following, a short overview of the CLEANER project[1] is provided with its main objectives and the necessary information for the deliverable D3.1 for which the University of Freiburg (UFR), *Inorganic Functional Materials and Nanomaterials Lab* headed by Prof. Dr. Anna Fischer, is a lead partner.

1.1 Context and Relevance

To achieve the European Green Deal's goal of making Europe the first climate-neutral continent by 2050, significant emission reductions are needed across all sectors of the economy, including power generation and heating. This challenge, coupled with the REPowerEU initiatives, highlights hydrogen's unique role as a clean energy carrier. Hydrogen can link various sectors, such as power and heat, transport, and industry and thereby offering benefits like long-term storage, long-distance transport, and production with little to no emissions. A cornerstone of the EU's climate strategy is the target to produce 10 million tons of renewable hydrogen domestically by 2030, complemented by an additional 10 million tons from imports. Achieving this will require extensive geological storage, a robust pipeline network, and comprehensive infrastructure to distribute hydrogen to end-users across Europe.

The primary goal of the CLEANER project is to design and operate a >100 kW polymer electrolyte membrane fuel cell (PEMFC) system using industrial-grade hydrogen for over 5,000 hours. This initiative aims to support the decarbonization of the power generation and heating sectors by leveraging highly efficient technology to deliver clean, zero-emission energy. As industrial-grade hydrogen contains various impurities, the need for impurity resistant and stable cathode as well as anode catalyst is of utmost importance.

The state-of-the-art PEMFC catalysts are predominantly based on Platinum (Pt). However, these catalysts have limited tolerance to impurities such as carbon monoxide (CO) and sulfur compounds, and they significantly contribute to the high capital expenses (CAPEX) of fuel cell systems. Enhancing CO tolerance at the anode can be achieved by designing HOR catalysts that exhibit reduced CO adsorption strength and/or improved CO electrooxidation activity. PtRu nanoalloys supported on carbon (PtRu/C) are a notable example, but their stability is compromised due to Ru dissolution[2].

As a more stable alternative, researchers have developed TiO_2- or M-doped TiO_2-supported Pt nanoparticles combined with carbon supports ($Pt/TiO_2/C$)[3], as well as emerging ultra-low-loading (single site) approaches. These catalysts demonstrate improved CO tolerance and electrochemical CO oxidation activity, as shown through rotating disk electrode (RDE) studies and single-cell measurements.

Additionally, catalyst activity can be recovered after impurity poisoning by cleaning the catalyst surface. Methods to restore activity include increasing the anode potential by altering the gas atmosphere to highly diluted H_2, directly raising the anode potential, or employing a combination

of both[4]. This process facilitates the oxidation of CO to CO_2 and sulfur to SO_2. However, the recovery process involves high potentials that can damage both anode and cathode catalysts. To address this, carbon supports resistant to electrochemical carbon corrosion must be designed and utilized.

The UFR will develop new catalysts based on hydrothermal N-doped carbon supports to improve both stability and activity for anode and cathode catalysts. For this purpose Nitrogen-doped hydrothermal carbon (N-HTC) supports previously developed by UFR and based on a low-cost, scalable, and sustainable hydrothermal carbonization (HTC) approach, starting from glucose, ovalbumine (egg-white protein) and water, yielding, after drying and pyrolysis, N-doped HTC aerogels, will further be optimized by UFR to serve as advanced catalyst supports in CLEANER.[5]

To implement a diagnostic functionality and be able to study electrochemical carbon corrosion events with high precision, ^{13}C-labeled N-HTC supports will be designed, in other words diagnostic twins. For this a fully ^{13}C-labeled carbon precursor will be used in the HTC process to yield fully ^{13}C-labeled N-HTC supports which will be used develop diagnostic Pt/C catalysts (optimized for ORR and CO-tolerant HOR) and implemented in catalyst layers, to be used in advanced diagnostic protocols at both single-cell and short-stack levels. Thereby the analysis of exhaust gases, in particular $^{13}CO_2$ will provide valuable information on the influence of operating conditions on operando carbon corrosion selectively occurring at the carbon support level.

1.2 Objectives

The main objective, to which UFR contributes, is the development of catalysts that can tolerate impurities in industrial-grade hydrogen while reducing overall catalyst costs. In detail, the development of catalyst for anode and cathode can be divided into three subtasks:

- **Development of novel carbon aerogel supports with high resistance against carbon corrosion and tuneable surface area and porosity. These will be ^{13}C-labeled, thereby allowing to develop advanced carbon corrosion diagnostics at the RDE, single cell and stack level. (D3.1)**
- Development of stable and carbon corrosion resistant catalysts both at the anode and cathode allowing the application of high potential recovery strategies to oxidatively free the catalyst surface from impurities.
- Development of stable CO tolerant catalysts at the anode able to operate at high levels of CO.

The following report summarizes the results related to the deliverable **D3.1 Stable N-HTC Carbon supports: "Synthesis, scaling and characterization of stable N-HTC carbon supports (non-labelled as well as ^{13}C-labeled) with enhanced resistance against carbon corrosion established."**

2. MATERIAL AND METHODS

All used chemicals and laboratory equipment for the development of novel carbon aerogel supports are described in the sections below. The hydrothermal synthesis is described as well as the used characterization methods relevant for carbon support development are presented.

2.1 Chemicals and equipment

All chemicals and equipment which were used for the synthesis and characterization of the Nitrogen-doped hydrothermal carbon materials (N-HTC) are listed in Table 1 below.

Table 1: Chemicals and equipment. *All used chemicals and equipment for the development of N-HTC materials are listed.*

Chemicals	**Comment**
H_2O (Milli-Q 18.2 MΩcm at 25°C)	
D-glucose (anhydrous, 96%)	
D-glucose (U-$^{13}C_6$, 99%)	
Ovalbumin	Different grades
Ethanol absolut >99,9% zur Analyse	
Reference carbon Vulcan®XC72R	

Equipment
Autoclave 45 mL
Autoclave 1000 mL
Tubular oven
Rotating tube furnace
Scanning electron microscope (SEM) FEG-HRSEM SU8220
Nitrogen physisorption (N2P) 3P micro 300
Elemental analysis Vario MICRO Cube system
X-Ray diffraction D8 Discover
Raman microscope SENTERRA II
TGA Thermogravimetrie Analyse Netzsch STA449 F5
EC-MS Elektrochemische Massenspektrometrie

2.2 General hydrothermal synthesis

Nitrogen-doped hydrothermal carbon materials (N-HTC) were synthesized following the method described previously by UFR in Martin et al.[5] In short, glucose and ovalbumin were dispersed in water and subjected to hydrothermal treatment in a Teflon-lined steel autoclave for several hours.

The resulting monolithic carbogel was washed and freeze-dried to preserve the aerogel structure. The dried product (yield: 30–40 wt.%) was then carbonized under an inert nitrogen atmosphere at 1000 °C to obtain nitrogen-doped hydrothermal carbon (N-HTC, yield: 40–50 wt.%).

For scale-up, precursor amounts were adjusted to a larger autoclave volume, and carbonization was carried out in a rotating tubular furnace under identical thermal conditions.

2.3 Characterization methods

The characterization methods used for the development of carbon support materials are listed below and a short description of the method is provided along with the necessity of the used method.

- **High-resolution scanning electron microscopy (HRSEM): Morphology**

High resolution scanning electron microscopy is a high-resolution imaging technique that uses a focused beam of electrons to scan the surface of a sample. During electron beam – sample interaction, different signals are emitted from the sample. When detecting emitted secondary electrons (SE) from the sample surface, detailed images of the sample topography / morphology with magnifications ranging from 100 to 500.000 times and point resolutions smaller than 2 nm can be obtained. When using emitted x-rays from the sample, the composition of the sample can be determined at different locations.

- **Nitrogen physisorption (N2P): Surface area / porosity**

Nitrogen physisorption is a widely used technique for characterizing the surface area and porosity of materials, particularly porous solids. It involves the physisorption of nitrogen gas molecules onto a sample's surface at cryogenic temperatures, typically 77 K (the boiling point of nitrogen). The process works by exposing the degassed sample to increasing/decreasing relative pressures of nitrogen while measuring the amount adsorbed. This data is used to generate adsorption-desorption isotherms, which provide valuable information about the material's porosity/texture, including, specific surface area (SSA), pore size distribution, pore volume (PV) and pore shape. Nitrogen physisorption is particularly useful for analyzing microporous (pore width <2 nm) and mesoporous (pore width 2–50 nm) materials. The technique is non-destructive and can be applied to a wide range of materials, from amorphous aluminosilicates to carbon-based materials. The Brunauer-Emmett-Teller (BET) method is commonly used to calculate the specific surface area from nitrogen physisorption data, although it may not be reliable for materials with very narrow micropores. To evaluate the Quenched Solid Density Functional Theory (QSDTF) analysis reveals a broad distribution of pore sizes

- **Elemental analysis (EA): Chemical composition / N-doping**

Elemental combustion analysis is a technique used to determine the elemental composition of organic compounds, particularly carbon, hydrogen, nitrogen, and sulfur. The sample is combusted at high temperatures (here: 1150 °C) in an oxygen-rich environment, converting the elements into

their oxidized forms (CO_2, H_2O, N_2, and SO_2). These combustion products are then separated and quantified using various detectors, such as thermal conductivity detectors or infrared spectroscopy. Results are typically indicated in wt%.

- **Powder X-ray diffraction (PXRD): Carbon microstructure / Graphitization degree**

Powder X-ray diffraction (XRD) is a non-destructive technique used to analyze the crystal structure, phase composition, and crystallinity of materials. It works by directing X-rays at a powdered sample and measuring the intensity of the diffracted X-rays at different angles. The resulting diffraction pattern provides information about the atomic structure of the material, allowing researchers to identify crystalline phases, determine lattice parameters, and estimate crystallite sizes. The XRD pattern of hexagonal graphite (2H graphite) is characterized by a dominant (002) reflection at approximately 26.5° 2θ (Cu Kα radiation), corresponding to the interlayer spacing of ~3.35 Å. This sharp and intense peak indicates the presence of well-ordered graphitic layers stacked along the c-axis. Additional reflections such as (100), (101), and (004) appear at higher angles, typically around 42–55° 2θ, and provide information about the in-plane structure and stacking order. The sharpness and intensity of these peaks reflect the degree of crystallinity and structural order in the graphite (carbon) sample.

- **Raman microscopy (Raman): Carbon microstructure / Graphitization degree**

Raman microscopy combines Raman spectroscopy with optical microscopy to provide chemical and structural information about materials at the microscopic level. It is based on the inelastic scattering of light by molecular vibrations. When a sample is illuminated with monochromatic light (usually from a laser), a small fraction of the scattered light undergoes a shift in frequency due to interactions with molecular vibrations. This "Raman shift" is characteristic of specific chemical bonds and molecular structures, allowing for the identification and analysis of materials at high spatial resolution. The Raman spectrum of carbon materials typically exhibits two prominent features: the *D* band around 1345 cm^{-1} and the *G* band near 1580 cm^{-1}. The *G* band arises from the in-plane vibrational modes of sp^2-hybridized carbon atoms and is common to all graphitic materials. In contrast, the *D* band is associated with structural disorder, edge effects, or defects within the graphitic lattice and becomes more pronounced as the degree of disorder increases. In highly ordered graphite or graphene, the *D* band is weak or absent. Additionally, a *2D* band (also known as the *G′* band) appears around 2700 cm^{-1} and provides insight into the number of graphene layers and stacking order.

- **Thermogravimetric analysis (TGA): Thermal stability**

Thermogravimetric analysis (TGA) is a thermal analysis technique that measures changes in the mass of a sample as a function of temperature or time in a controlled atmosphere. The sample is heated at a constant rate while its mass is continuously monitored using a precise balance. TGA provides information about thermal stability, decomposition temperatures, moisture content, and the composition of materials. It is particularly useful for studying materials that undergo weight changes due to decomposition, oxidation, or dehydration processes.

- **Electrochemical-coupled mass spectrometry (EC-MS): Carbon support stability in electrochemical carbon corrosion**

EC-MS by Spectro Inlets is a turnkey solution for real-time mass spectrometry analysis of electrochemical reactions. The system combines electrochemistry with mass spectrometry, allowing researchers to study volatile substances produced during electrochemical processes.[6]

3. DEVELOPMENT OF HYDROTHERMAL CARBON SUPPORTS

This section deals with the synthetic procedures and material characterization of the hydrothermal carbon materials. The experimental results of the different tasks, synthesis and scaling of the N-HTC carbon supports, tuning of graphitization degree, synthesis of high surface area (HSA) carbon supports, cost reduction via the use of lower grade precursors and implementation of ^{13}C-labeling are presented. The examination of the resistance against carbon corrosion of the developed materials is provided in chapter 4. Further, a detailed comparison of the different N-HTC materials is summarized in chapter 5.

3.1 Synthesis of Nitrogen-doped hydrothermal carbon supports (N-HTC) in small scale

Nitrogen-doped hydrothermal carbon supports (N-HTC) were synthesized as previously reported by UFR according to Martin et al.[5] and the description in section 2.2. The resulting samples were carbonized at 1000 °C and were characterized with the described methods in section 2.3 to evaluate their morphology, microstructure and composition and evaluate their applicability as a carbon supports for later electrocatalyst design. First, the synthesis was done in a small-scale batch to check reproducibility and to obtain a baseline material for the upscaling process. The morphology of the newly synthesized N-HTCs is comparable with those reported in literature.[5,7] The characteristic coral-like structure of the N-HTC carbon support was revealed by SEM as seen in Figure 1.

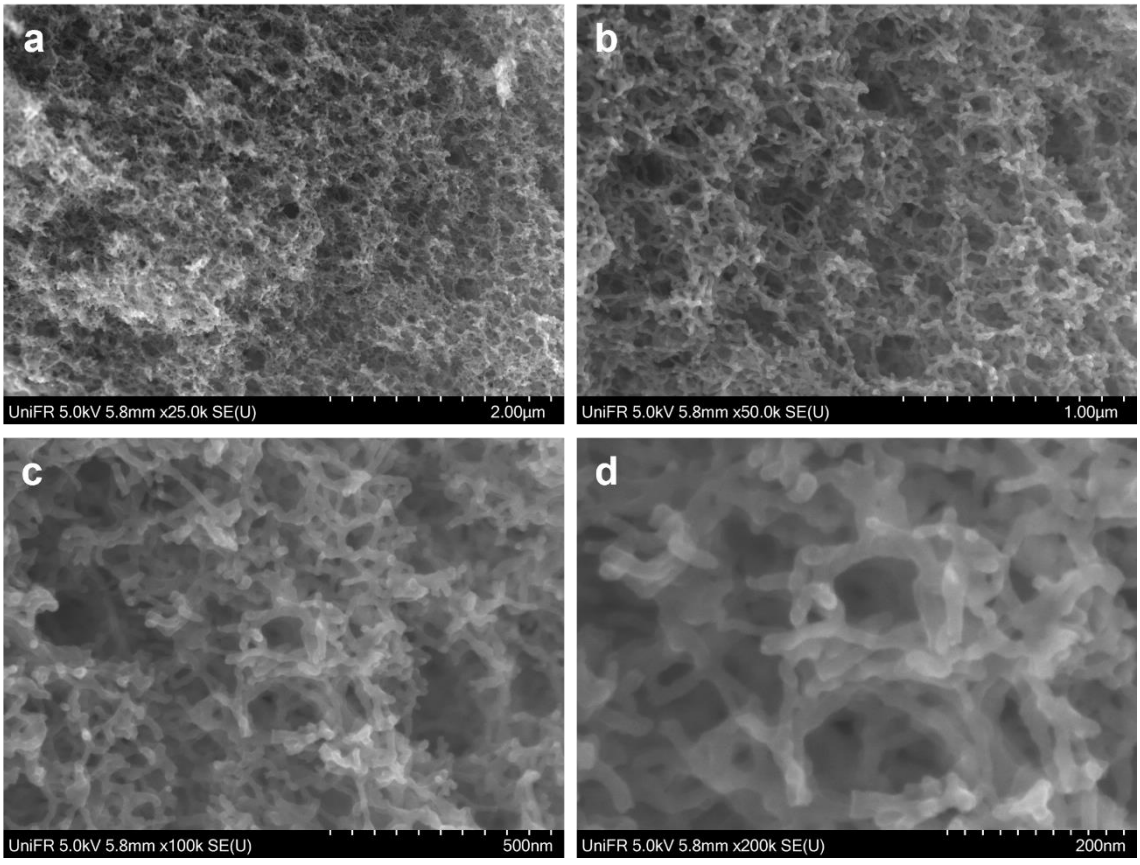

Figure 1: SEM micrographs of small-scale N-HTC. *a – d) SEM micrographs of small-scale N-HTC with different magnifications.*

The porous characteristics of the N-HTC supports, including BET surface area, pore volume, and pore size distribution, were assessed through N_2 physisorption measurements at 77 K. The N-HTC samples display a pore size distribution, which corresponds well with their morphology. The SSA_{BET} accounts for (277±28) $m^2\,g^{-1}$ and is comparable with literature.[5,7] Quenched Solid Density Functional Theory (QSDTF) analysis reveals a broad distribution of pore sizes, with a maximum around 1 nm in the microporous range (Figure 2b). The total pore volume of (0.44±0.05) $cm^3\,g^{-1}$ is primarily contributed by mesopores between 2 and 30 nm, whereas micropores account for only a smaller fraction (<20 %, see Table 2).

The elemental bulk composition of the synthesized N-HTC materials was determined via elemental combustion analysis (C, H, N, S) and the results are summarized in Figure 2c. The oxygen content was calculated by assuming that the residual wt.% after subtraction of the C, H, N, S wt%. The N-HTC carbon the chemical bulk composition consists of ~90 wt.% carbon and ~2 wt.% nitrogen, revealing the heteroatom doping for these materials in contrast to the commonly used carbon blacks, e.g. Vulcan XC72R, which mainly consist of carbon ~98 wt.% (Appendix A. Figure 13).

X-Ray diffraction (Figure 2d) shows typical features for carbon materials. The XRD patterns can be attributed to the (002), (100)/(101) and (110) reflections of hexagonal graphite (P63/mmc). The broad signals indicate a semi-crystalline structure, as expected for hydrothermal carbon materials treated at ~1000 °C.

All samples exhibit broadened Raman signals (Figure 2e) compared e.g. to graphite, suggesting a higher content of amorphous carbon and the presence of structural defects in the carbon matrix.[8] The N-HTC sample shows a so-called *D* band at 1345 cm^{-1} and the *G* band at 1580 cm^{-1} and the 2*D* band in the range of 2400–3000 cm^{-1}, which is associated with second-order Raman scattering. The Raman spectra were analyzed using a five-band fitting model with mixed Gaussian/Lorentzian peak shapes (Figure 2e). In highly disordered carbon nanostructures, in addition to the *G* band (E_{2g} symmetry, corresponding to in-plane vibrations of an ideal hexagonal graphite lattice) and the *D1* band (A_{1g} symmetry, linked to lattice disorder), three additional disorder-induced *D* bands can be identified: *D4* at 1210 cm^{-1}, *D3* at 1530 cm^{-1} and *D2* at 1604 cm^{-1}.[9] Together with the XRD results, the N-HTC material can be identified as a semi-crystalline carbon material.

To investigate the thermal behaviour and combustion stability of the N-HTC materials, thermogravimetric analysis (TGA) was conducted. The samples were heated in air up to 900 °C, and the resulting mass loss as a function of temperature is presented in (Figure 2f). The onset of combustion is around 520 °C. Compared to a standard carbon material (Vulcan XC72R, Appendix A. Figure 13) with a T_{onset} around 595 °C, the thermal stability is a little bit lower.

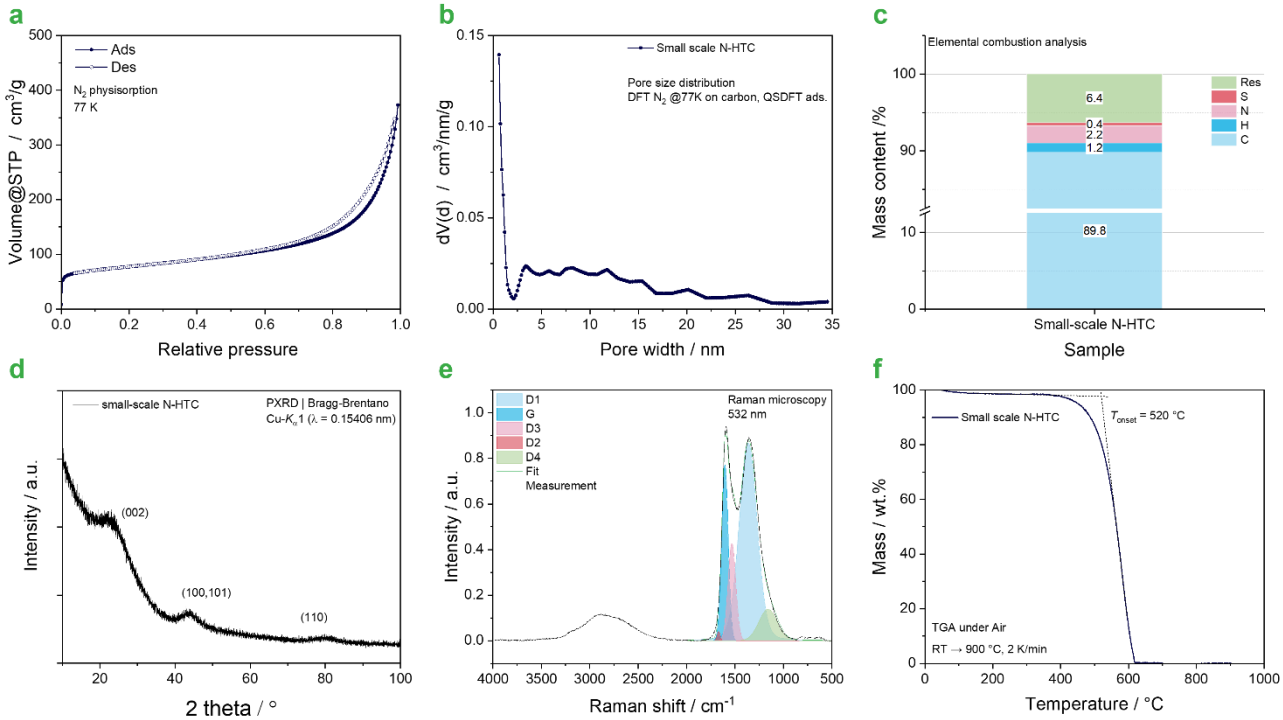

Figure 2: Small-scale N-HTC characterization. *a) Nitrogen physisorption isotherm and b) Pore size distribution (DFT model). c) Elemental combustion analysis. d) Powder X-Ray diffraction. E) Raman microscopy and 5-peak fit. f) TGA measurement under air.*

3.2 Synthesis of Nitrogen-doped hydrothermal carbon supports (N-HTC) in large scale

The N-HTC synthesis was upscaled to larger batch sizes to provide sufficient support material for catalyst synthesis and scaling as well as MEA fabrication (WP4, PowerCell), single-cell and short-stack testing (WP4, WP5, SINTEF, VTT).

Therefore, the synthesis was carried out in a larger autoclave volume, whereas the synthesis parameters were kept unchanged. First attempts of the large-scale synthesis revealed in Nitrogen-physisorption measurements (Appendix A. Figure 14) a smaller surface area for the non-optimized large-scale N-HTC support of ~100 $m^2\ g^{-1}$ in contrast to small-scale N-HTC support of ~277 $m^2\ g^{-1}$ (Figure 2). The carbon (micro)structure, investigated via XRD and Raman microscopy measurements, showed no significant differences between small- (Figure 2) and large-scale N-HTC supports (Appendix A. Figure 14).

We attribute this finding to a scaling effect, which was investigated by tuning the synthesis procedure while maintaining all experimental parameters constant to ensure consistency between small- and large-scale batches. When controlling the synthesis parameters very thoroughly, the N-HTC synthesis was upscaled successfully to larger batch sizes.

The porous characteristics of the optimized large-scale N-HTC supports, morphology investigated via SEM (Figure 3) and BET surface area, pore volume, and pore size distribution (Figure 4) were comparable to the small-scale N-HTC samples, while the carbon (micro)structure (XRD, Raman microscopy) still showed no significant differences between small- and large-scale N-HTC supports.

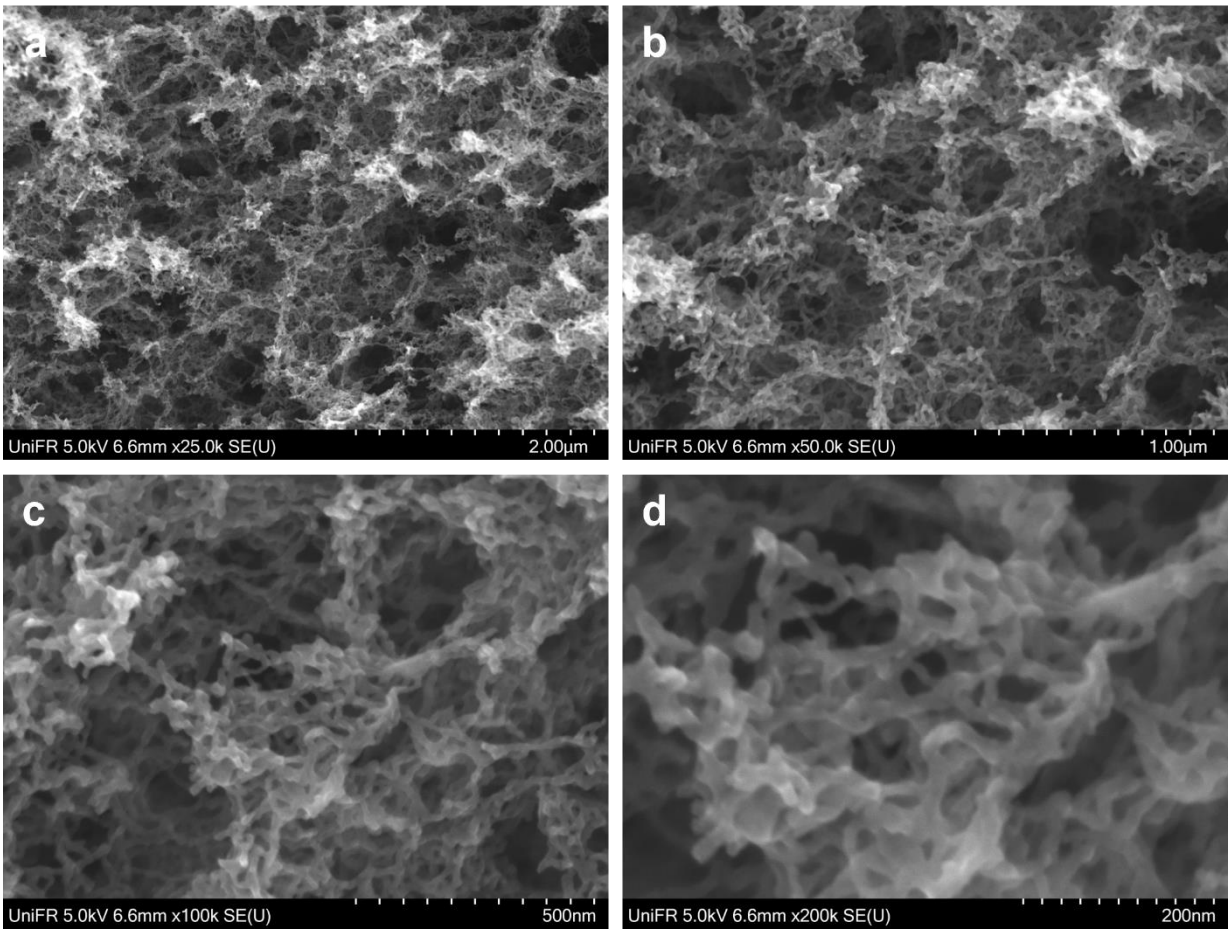

Figure 3: SEM micrographs of optimized large-scale N-HTC. *a – d) SEM micrographs of large-scale N-HTC with different magnifications.*

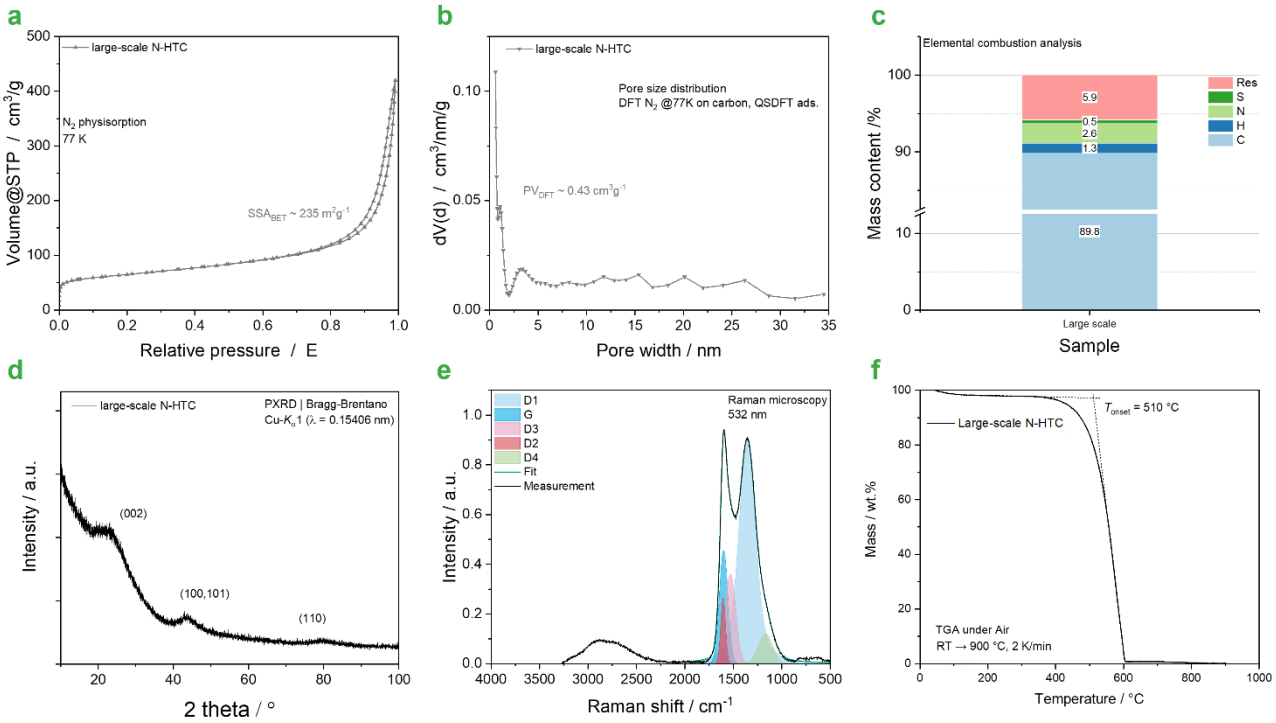

Figure 4: Large-scale N-HTC characterization. *a) Nitrogen physisorption isotherm and b) Pore size distribution (DFT model). c) Elemental combustion analysis. d) Powder X-Ray diffraction. e) Raman microscopy and 5-peak fit. f) TGA measurement under air.*

3.3 Tuning of graphitization degree

Based on our previous work (Martin et al.[5]), in which N-doped hydrothermal carbon aerogels (N-HTC) were investigated as supports for Pt-based oxygen reduction reaction (ORR) electrocatalysts, the materials were initially pyrolyzed at different temperatures (900 °C, 1000 °C, and 1500 °C) under inert atmosphere. The resulting samples were structurally characterized with respect to porosity, elemental composition, surface functionalization, crystallinity, and electrical conductivity.

Building on this work and aiming to further enhance the stability of the N-HTC materials towards carbon corrosion, additional high-temperature treatments were applied. Specifically, N-HTC samples were heated to temperatures in the range of 1000 °C–1700 °C (*T*1–*T*3).

In Figure 5 the characterization of these materials is shown. The X-Ray diffraction (Figure 5a) shows typical features for carbon materials. With higher graphitization temperature, the signals get narrower and more distinct, indicating that the semi-crystalline structure becomes more and more crystalline with higher temperatures. This behaviour is in line with previous results [5] and confirmed by Raman spectroscopy measurements (Figure 5b). The Raman signals of the N-HTC samples show the typical *D* band at 1345 cm^{-1} and the *G* band at 1580 cm^{-1} and the 2*D* band in the range of 2400–3000 cm^{-1}, which is associated with second-order Raman scattering. These become more distinct for the higher graphitized samples. Although precise quantification of

amorphous content and in-plane crystallite size remains challenging, the peak deconvolution results reveal (Figure 5d) that, with increasing pyrolysis temperature, the relative areas of the *D3* and *D4* bands, associated with amorphous carbon and trans-polyacetylene-like structures at graphitic edges, decrease. In contrast, the intensities of the *D1*, *D2*, and *G* bands increase, reflecting a higher degree of carbonization and structural ordering.

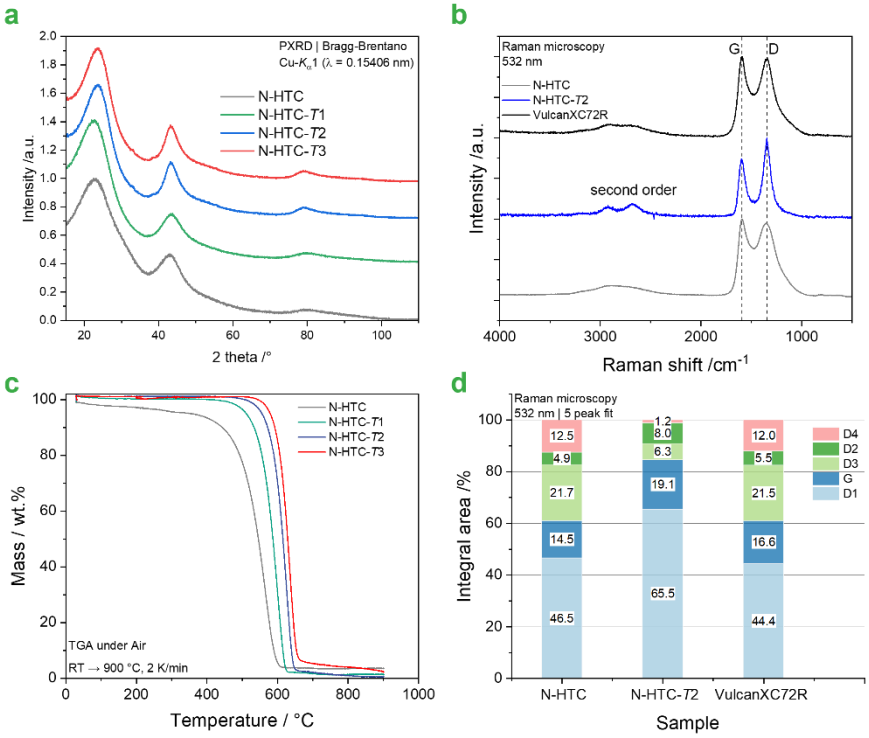

Figure 5: Graphitization N-HTC characterization. *a) Powder X-Ray diffraction. b) Raman microscopy c) TGA measurement under air. e) Raman microscopy 5-peak fit.*

With increased graphitization degree, an increase in thermal stability is observed (Figure 5c). The onset of combustion is around 520 °C for the N-HTC-1000 and rises to >600 °C for N-HTC-1700, exceeding the thermal stability of a standard carbon material (Vulcan XC72R, Appendix A. Figure 14) with a T_{onset} around 595 °C. This behaviour indicates also an increase in carbon corrosion resistance, which is covered in section 4.1.

3.4 Synthesis of high surface area (HSA) carbon supports

The surface area of the N-HTC carbons was increased by activation to yield high surface area carbon (HSAC) supports (>500 m^2/g), allowing to fine tune the micro/mesopore ratio of the N-HTC. The HSAC materials were synthesized via physical/chemical activation methods.

The untreated N-HTC material is compared with an activated N-HTC material of the same batch and is denoted as N-HTC-HSA. Investigations via SEM reveal that no visual changes can be observed, and that the coral-like aerogel structure is preserved upon activation (Figure 6).

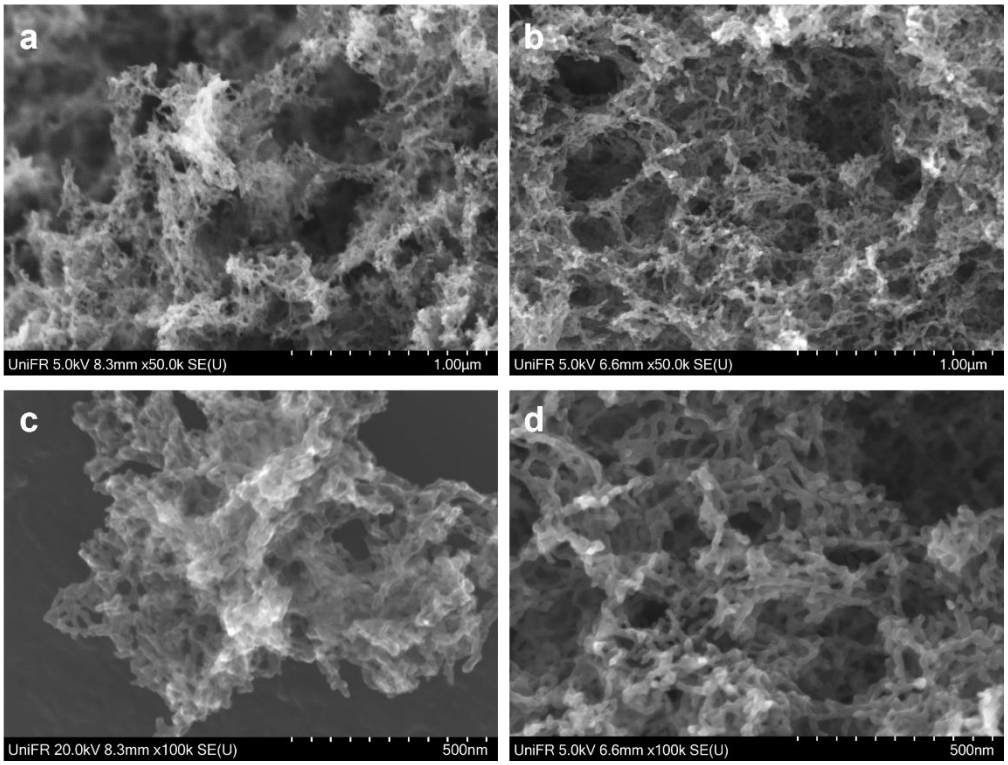

Figure 6: SEM micrographs of N-HTC-HSA. *a)+c) SEM micrographs of an activated N-HTC-HSA and b)+d) conventional N-HTC. The coral-like structure is preserved upon activation and no visual changes can be observed.*

A comparison of the isotherms reveals that the activated material exhibits a significantly greater increase in microporosity, approximately twice as pronounced as that observed in the isotherm of the non-activated N-HTC (Figure 7). Beyond this initial increase, the overall shape of the isotherms remains largely unchanged, which aligns with expectations following carbon activation. Activation primarily promotes the formation of micropores in the system. As a result, the relative contribution of micropores to the surface area has increased from 80% to over 90%, while their share of the total pore volume has nearly doubled, rising from ~20% to 40%.
Notably, the activation process only slightly affects the elemental composition, the carbon microstructure (XRD and Raman) or the thermal stability of the sample (Figure 7).

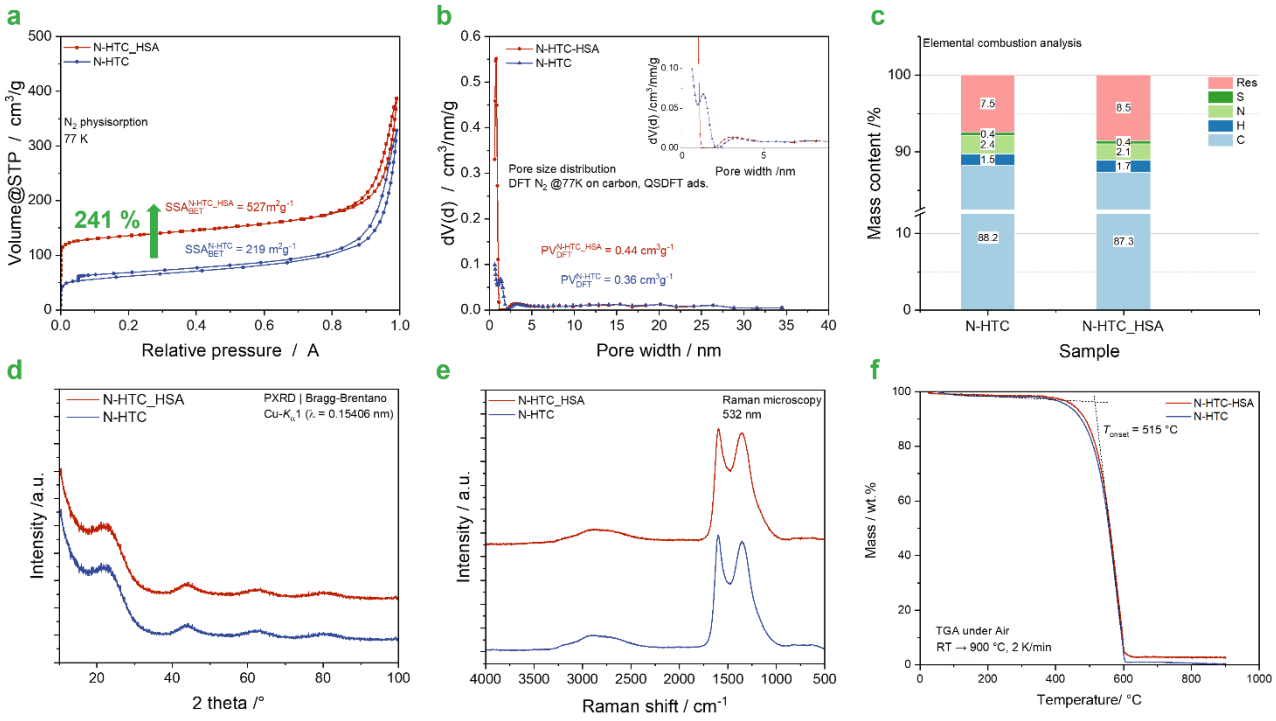

Figure 7: N-HTC-HSA characterization. *a) Nitrogen physisorption isotherm and b) Pore size distribution (DFT model). c) Elemental combustion analysis. d) Powder X-Ray diffraction. E) Raman microscopy and 5-peak fit. f) TGA measurement under air.*

3.5 Cost reduction via the use of lower grade precursors

To reduce the costs of the carbon support material, the influence of the ovalbumine grade on the resulting 3D N-HTC morphology and structure was investigated, with the aim to use the lowest grade possible, while maintaining the porous properties.

The synthesis procedure remained the same as for the standard N-HTC material. Different grades of precursor, corresponding to different purities, were used.

In Figure 8 the SEM micrographs of different N-HTC samples with different ovalbumin grades are shown. Compared to the standard N-HTC, the different grades show a slightly different structure. The samples N-HTC with lower purity lack the well-defined coral-like architecture, desirable for the use as carbon support material for metal nanoparticles.

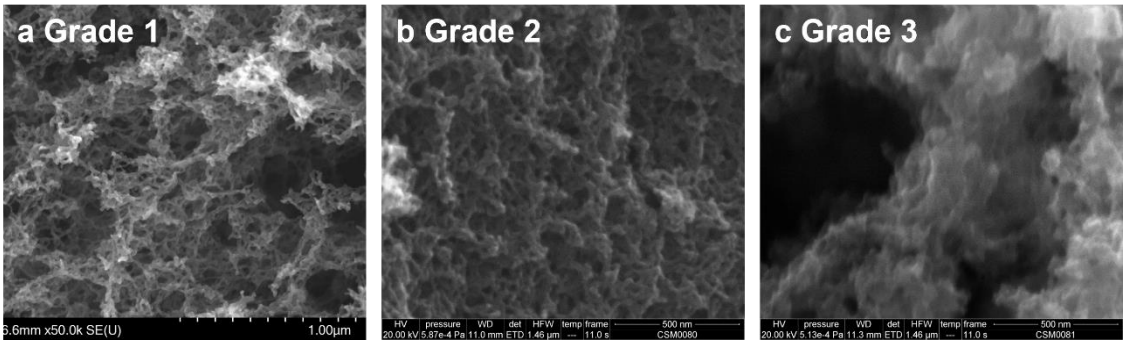

Figure 8: SEM micrographs of different albumin grade N-HTC.

While the morphology of the samples changes, the samples exhibit a nearly identical elemental composition. Importantly, the different albumin grades have no significant impact on the carbon microstructure (as confirmed by XRD and Raman spectroscopy). Also, the thermal behaviour of the samples is almost identical.

While the lower-grade precursors still produce porous carbon materials with comparable surface areas and pore volumes (as determined by N_2-physisorption), they lack the well-defined coral-like architecture desirable for certain applications (and only measurably by quicksilver porositmetry). Nonetheless, these materials remain of interest, as their carbon microstructure, thermal stability (indicative of resistance to carbon corrosion), and nitrogen content are comparable to those of the standard reference material N-HTC-Albumin-GradeV made with a higher quality albumin.

For future investigations, it will be essential to explore the scalability of these lower-grade albumin derived-carbon materials to assess their viability as cost-effective alternatives for the production of functional carbon supports.

3.6 Implementation of ^{13}C labeling

To implement a diagnostic functionality and be able to study carbon corrosion events in detail, fully ^{13}C-labeled glucose was used as carbon precursor in the HTC process to yield fully ^{13}C-labeled N-HTC as diagnostic supports.

The results of this labeling approach have been published in the journal *Advanced Energy Materials*: N. Ortlieb‡, J. Martin‡, L. Guggolz, J. Ihonen, and A. Fischer*, ^{13}C-Labeled Mesoporous N-Doped Carbon Nanospheres and N-Doped Hydrothermal Carbon Aerogels as Model Materials for Carbon Corrosion Determination in Electrode Structures, *Adv. Energy Mater*. 2025, 2406164. https://doi.org/10.1002/aenm.202406164.[10]

‡ *N. Ortlieb and J. Martin contributed equally to this work.*

In this study, the developed hydrothermal N-doped carbon (N-HTC) materials, were used as model carbon support materials to investigate the impact of ^{13}C-labeling on the physicochemical properties of carbon supports. Materials with varying degrees of ^{13}C-incorporation, as well as physical mixtures of unlabeled and fully labeled samples, were examined in EC-MS studies under accelerated carbon stress test (AST) conditions to assess how ^{13}C-labeling influences the detection of $^{12}CO_2$ and $^{13}CO_2$, key products of carbon corrosion.

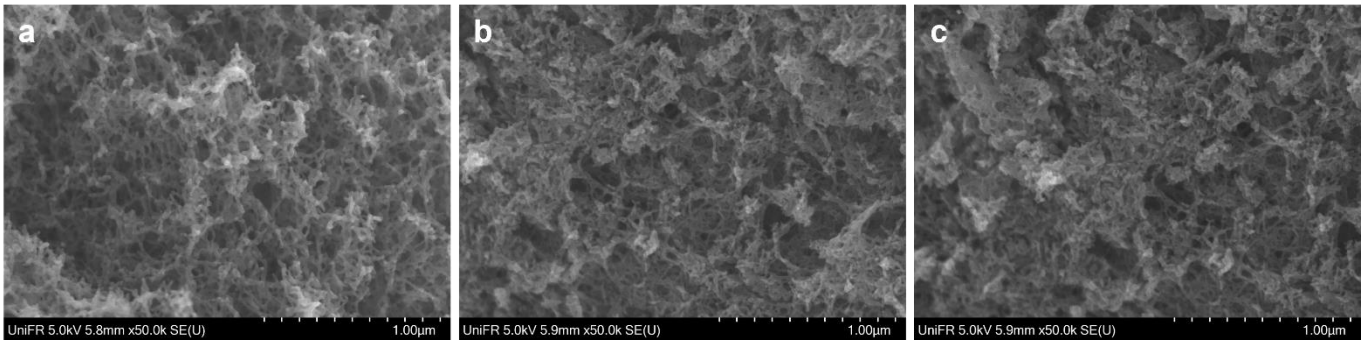

Figure 9: SEM micrographs of isotope ^{13}C-labeled N-HTC. *a) SEM micrographs of small-scale non-labeled N-HTC, b) 50:50 mixture and c) fully ^{13}C-labeled N-HTC.*

For N-HTC, the material characterization is shown in Figure 9 and Figure 10. The SEM micrographs (Figure 9) of non-labeled N-HTC, 50:50 mixture and fully ^{13}C-labeled N-HTC only show slight variations in their morphology. Additionally, the material characteristics of the different non-labeled N-HTC and ^{13}C-labeled N-HTC (Figure 11) show very comparabel results. The BET surface area ranges from 306 $m^2\,g^{-1}$ to 273 $m^2\,g^{-1}$ (Figure 11a) and the chemical compoistion is almost identical (Figure 11c). The microstructure (XRD and Raman) again shows no major difference to the unlabeled materials described. The only visible difference is related to the position of the Raman bands of the labeled materials, related to the isotopic effect.

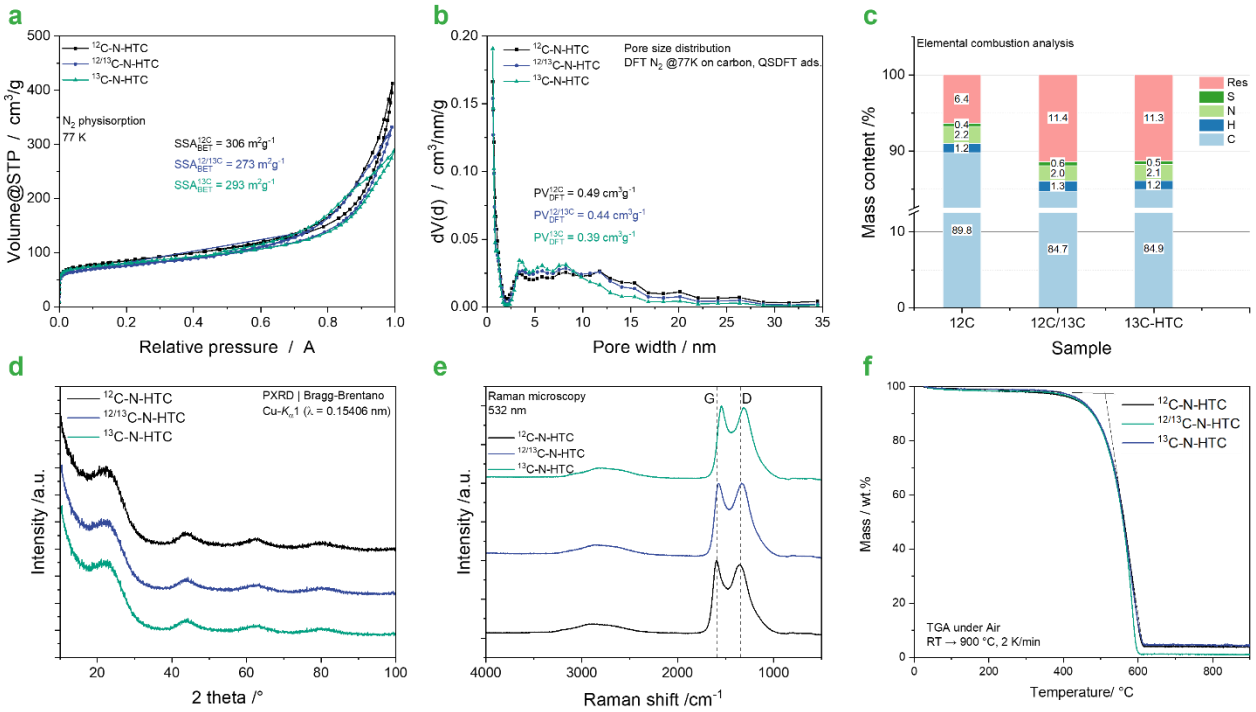

Figure 10: Isotope ^{13}C-labeled N-HTC characterization. *a) Nitrogen physisorption isotherm and b) Pore size distribution (DFT model). c) Elemental combustion analysis. d) Powder X-Ray diffraction. E) Raman microscopy. f) TGA measurement under air.*

In summary, we demonstrate that ^{13}C-labeling of N-HTC can be achieved without affecting their morphology or physicochemical characteristics. These ^{13}C-labeled materials can serve as diagnostic carbon twins in a range of electrochemical applications, such as in situ $^{13}CO_2$ tracking (see section 4.2) of catalyst support degradation in PEM fuel cells, or in studies of electrode and additive degradation in supercapacitors and battery systems.

4. CARBON CORROSION

Carbon materials are generally chemically inert, a property that enhances the longevity and stability of electrochemical energy devices. However, in harsh oxidative electrochemical environments, carbon can undergo corrosion or degradation into CO_2 (and CO), primarily due to electrochemical oxidation:

$$C + 2H_2O \rightarrow CO_2 + 4H^+ + 4e^- \qquad E^0 = 0.207 \text{ V vs. RHE} \qquad \text{(Eq. 1)}$$

$$C + H_2O \rightarrow CO + 2H^+ + 2e^- \qquad E^0 = 0.518 \text{ V vs. RHE} \qquad \text{(Eq. 2)}$$

These reactions kinetically take place at elevated oxidative potentials, with particularly high anodic potentials above 0.8 V vs. RHE (reversible hydrogen electrode) significantly accelerating carbon corrosion.[11] Elevated temperatures and the presence of confined water further increase corrosion rates.[12] In proton exchange membrane fuel cells (PEMFCs), carbon corrosion can result in the degradation of the catalyst support, leading to a reduction in the electrochemically active surface area and electrode shrinkage, ultimately diminishing overall cell performance and lifespan.[13]

To study the carbon corrosion resistance of the developed N-HTC materials, electrochemically coupled mass spectrometry method (SpectroInlets) was used. In short, the carbon supports were dispersed in an alcohol/water mixture and homogenized with an ultrasonic horn sonifier to prepare a stable ink. The ink was drop-casted on a glassy carbon electrode (GC) to achieve a thin carbon material coating which was mount in the measuring cell. By applying a potential to the working electrode, the responding current and the responding mass current of the detected species in the mass spectrometer were monitored to evaluate the carbon corrosion (CO_2 signal).

4.1 Enhancing stability via graphitization of N-HTC materials

To assess the carbon corrosion resistance stability of N-HTC materials, the samples carbonized/graphitized at different temperatures (*T*1–*T*3), presented in section 3.3, were examined via EC-MS measurements.

In Figure 11a the measurement protocol of the EC-MS characterization is shown. The working electrode is polarized up to 1.4 V vs. RHE to start the carbon corrosion. With the EC-MS it is possible to detect any signals of decomposition products during the electrochemical measurements. In Figure 11b–d the corresponding mass spectra of CO_2 signal of b) standard N-HTC material carbonized at 1000°C and c) graphitized N-HTC material and a reference carbon material Vulcan XC72R are shown. No CO_2 can be detected at 1.4 V vs. RHE for the high temperature (-*HT*) N-HTC-*HT* material, confirming a higher carbon corrosion resistance. When going to higher potentials (1.7 V vs. RHE) also the higher graphitized samples begin to corrode and form CO_2.

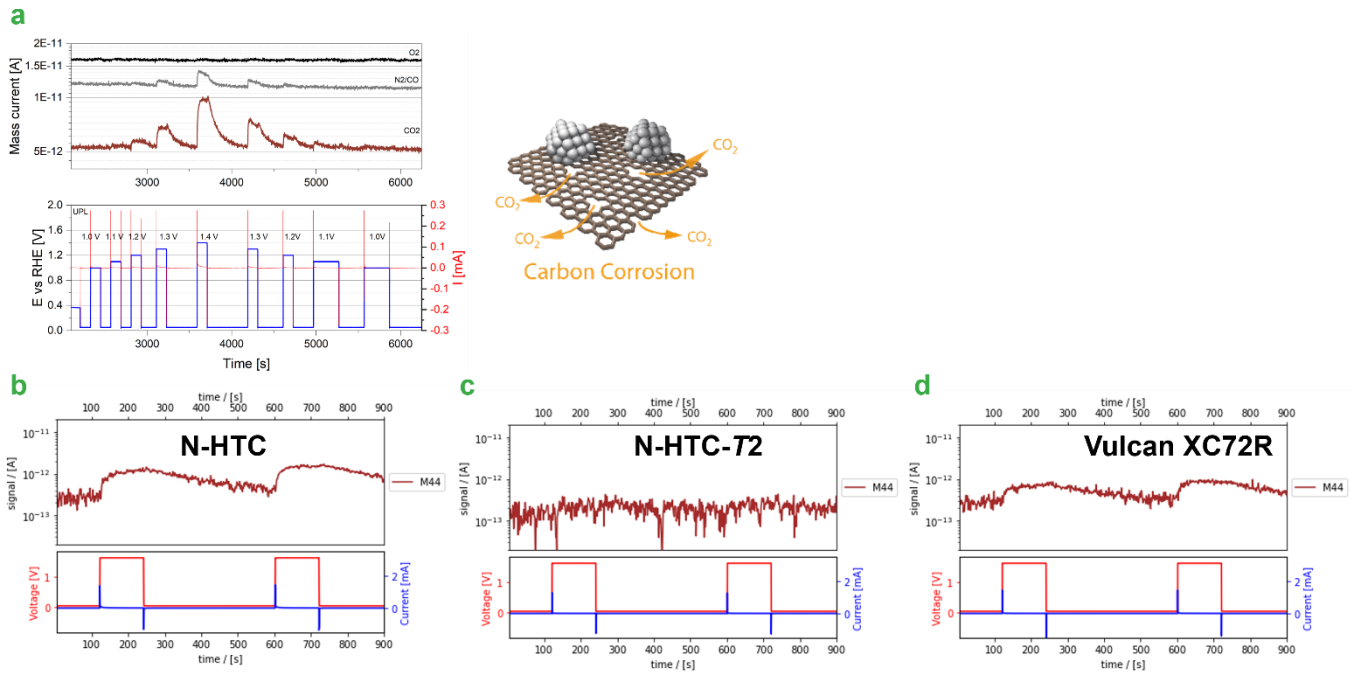

Figure 11: Carbon corrosion measurements of graphitized N-HTC. *a) Example of a potential and responding current shape for an increasing square wave potential from 0.05 to 1.40 V vs. RHE with mass current signals of CO_2 (m/z = 44), N_2/CO (m/z = 28), O_2 (m/z = 32) and carbon corrosion. Corresponding mass spectra of CO_2 signal of b) standard N-HTC material carbonized at 1000°C and c) graphitized N-HTC material and a reference carbon material Vulcan XC72R (Cabot Corporation).*

4.2 Implementation of ^{13}C labeling

To prove the incorporation of ^{13}C-labeling and to assess how ^{13}C-labeling influences the detection of $^{12}CO_2$ and $^{13}CO_2$, the N-HTC materials (section 3.6) with varying degrees of ^{13}C, as well as physical mixtures of unlabeled and fully labeled samples, were examined in EC-MS studies under accelerated carbon stress test (AST) conditions.[10]

Figure 12 illustrates the carbon corrosion measurements of ^{13}C-labeled N-HTC and an unlabeled (^{12}C N-HTC) sample. By applying a potential to the working electrode, the responding current and the responding mass current of the detected species in the mass spectrometer were monitored to evaluate the carbon corrosion (CO_2 signal). The working electrode is polarized to 1.7 V vs. RHE to start the carbon corrosion. For the unlabelled N-HTC sample (Figure 12b) a molecule with the mass 44, which we attribute to $^{12}CO_2$ and for the ^{13}C-labelled N-HTC sample (Figure 12bc) a molecule with the mass 45, corresponding to $^{13}CO_2$, could be detected. Thereby we could confirm the ^{13}C-labelling of N-HTC support.

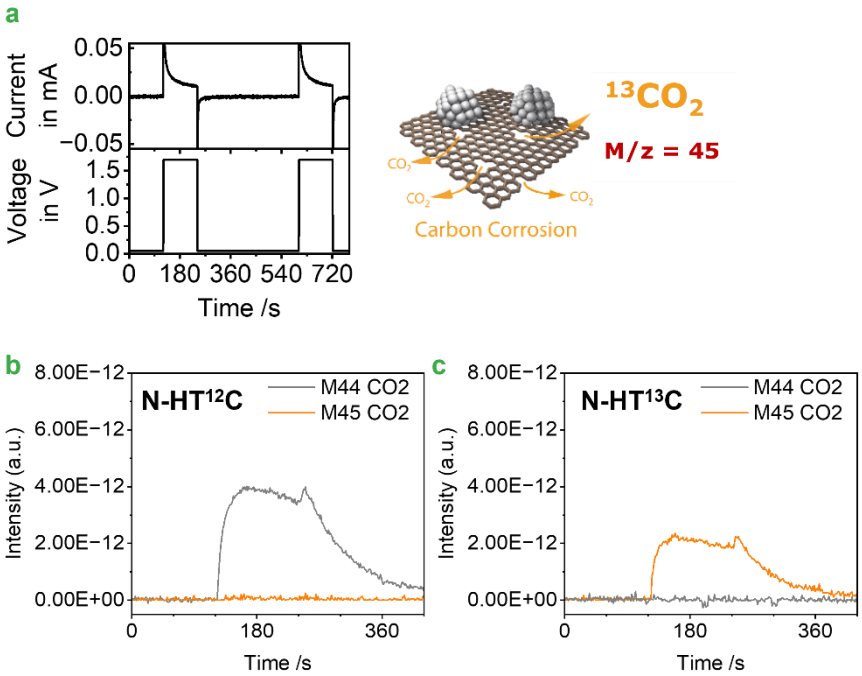

Figure 12: Carbon corrosion measurements of ^{13}C-labeled N-HTC. *a) Potential and responding current shape for a square wave potential from 0.05 to 1.70 V vs. RHE and carbon corrosion illustration with $^{13}CO2$ with 45 mass number. Corresponding mass spectra of b) non-labeled N-HT^{12}C sample and c) ^{13}C-labeled N-HT^{13}C sample with detection of CO_2 with mass number 44 ($^{12}CO_2$) and 45 ($^{13}CO_2$).*

5. SUMMARY OF WORK AND CONCLUSIONS

In Table 2 the material properties of the different N-HTC carbon supports are summarised. We successfully synthesized, scaled, modified and characterized non-labeled as well as ^{13}C-labeled N-HTC carbon supports (D3.1 Stable N-HTC Carbon supports). In detail

- Upscaling of N-HTC synthesis
- Increase of carbon corrosion resistance
- Increase of surface area by activation
- Reducing costs by lower grade precursors
- Implement diagnostic functionality by employing a ^{13}C-labeling

Table 2: Summary of material characteristics of N-HTC samples. *The various samples of N-HTC materials presented in chapter 3 are summarized here. The most important material characteristics which qualify for the application as electrocatalyst support are presented.*

Sample	[a]SSA^{BET}	[b]PV^{DFT}	[c]PV_{Meso}	[d]*C* cont.	[e]*N* cont.	[g]T^{TGA}
	m^2g^{-1}	cm^3g^{-1}	%	wt.%	wt.%	°C
Small-scale N-HTC	277±28	0.44±0.05	82±1	90	2.2	520
Large-scale N-HTC	235±14	0.43±0.06	82±4	90±2	2.6±0.2	510
N-HTC-*HT*	178	0.53	90	99	0.2	>600
N-HTC-HSA	527	0.42	60	87	2.1	515
N-HTC-grade3	273	0.59	90	87	4.2	580
N-HTC-fully-^{13}C	273	0.44	83	85	2.0	
N-HTC-50:50-^{13}C	293	0.39	79	85	2.1	
Vulcan XC72R	226	0.31	76	98	-	595

a Specific surface area **b** Total pore volume **c** Mesopore (2–50 nm pore diameter) pore volume fraction **d** Carbon content and **e** Nitrogen content determined via EA combustion analysis. **f** Onset temperature via TGA.

The upscaling of the N-HTC carbon support was successfully established. The same material properties can be found for the small-scale N-HTC (yield ~0.3 g per batch) and the large-scale N-HTC (yield ~9 g per batch). The morphology, BET surface area and the carbon (micro)structure, investigated via XRD and Raman microscopy measurements, showed no significant differences between small- and large-scale N-HTC supports.

The examination of the **resistance against carbon corrosion** of the developed materials showed that the graphitization was successful in stabilizing the carbons against corrosion.

The surface area of the N-HTC carbons was increased by activation to yield high surface area carbon (HSAC) supports (>500 m^2/g), allowing to fine tune the micro/mesopore ratio of the N-HTC.

Trying to reduce the costs of the N-HTC material by using lower-grade precursors still produced porous carbon materials with comparable surface areas and pore volumes. Despite lacking the well-defined coral-like architecture desirable for certain applications, these materials remain of

interest, as their carbon microstructure, thermal stability (indicative of resistance to carbon corrosion), and nitrogen content are comparable to those of the standard reference material N-HTC.

^{13}C-labeling of N-HTC was successfully implemented without altering the morphology or physicochemical properties of the N-HTC supports. These labelled materials function as diagnostic carbon twins, enabling applications such as in situ $^{13}CO_2$ tracking of catalyst support degradation in PEM fuel cells (see section 4.2).

In summary, we successfully scaled up the synthesis of nitrogen-doped hydrothermal carbon (N-HTC) to larger batch sizes, ensuring a sufficient supply of carbon support material. Additionally, we optimized the degree of graphitization, which led to enhanced stability of the carbon materials against corrosion. Furthermore, we implemented diagnostic functionality by employing a ^{13}C-labeled glucose precursor. This enabled the production of fully ^{13}C-labeled N-HTC diagnostic supports, allowing for detailed studies of carbon corrosion processes.

In the framework of the CLEANER project, the developed nitrogen-doped hydrothermal carbon (N-HTC) materials will serve as advanced carbon supports for both anode and cathode catalysts. As stable cathode (anode) catalysts, particularly the more corrosion-resistant N-HTC carbon supports are of interest, while the high-surface area N-HTC materials are promising alternatives for the development of CO-resistant anode. The ^{13}C-labeld N-HTC materials will serve as a diagnostic material for Pt-based cathode catalysts.

6. BIBLIOGRAPHY

(1) *"CLEANER - Clean heat and Power from Hydrogen," 2024. [Online]. Available: https://www.cleaner-h2project.eu/ [Accessed 02.12.2024]*.

(2) Molochas, C.; Tsiakaras, P. Carbon-Monoxide-Tolerant Pt-Based Electrocatalysts for H2-Pemfc Applications: Current Progress and Challenges. *Catalysts* **2021**, *11* (9). https://doi.org/10.3390/CATAL11091127.

(3) Antoniassi, R. M.; Quiroz, J.; Barbosa, E. C. M.; Parreira, L. S.; Isidoro, R. A.; Spinacé, E. V.; Silva, J. C. M.; Camargo, P. H. C. Improving the Electrocatalytic Activities and CO Tolerance of Pt NPs by Incorporating TiO2 Nanocubes onto Carbon Supports. *ChemCatChem* **2021**, *13* (8), 1931–1939. https://doi.org/10.1002/CCTC.202002066.

(4) Li, Z.; Wang, Y.; Mu, Y.; Wu, B.; Jiang, Y.; Zeng, L.; Zhao, T. Recent Advances in the Anode Catalyst Layer for Proton Exchange Membrane Fuel Cells. *Renewable and Sustainable Energy Reviews* **2023**, *176*, 113182. https://doi.org/10.1016/J.RSER.2023.113182.

(5) Martin, J.; Melke, J.; Njel, C.; Schökel, A.; Büttner, J.; Fischer, A. Electrochemical Stability of Platinum Nanoparticles Supported on N-Doped Hydrothermal Carbon Aerogels as Electrocatalysts for the Oxygen Reduction Reaction. *ChemElectroChem* **2021**, *8* (24), 4835–4847. https://doi.org/10.1002/celc.202101162.

(6) Trimarco, D. B.; Scott, S. B.; Thilsted, A. H.; Pan, J. Y.; Pedersen, T.; Hansen, O.; Chorkendorff, I.; Vesborg, P. C. K. Enabling Real-Time Detection of Electrochemical Desorption Phenomena with Sub-Monolayer Sensitivity. *Electrochim Acta* **2018**, *268*, 520–530. https://doi.org/10.1016/J.ELECTACTA.2018.02.060.

(7) White, R. J.; Yoshizawa, N.; Antonietti, M.; Titirici, M.-M. A Sustainable Synthesis of Nitrogen-Doped Carbon Aerogels. *Green Chemistry* **2011**, *13* (9), 2428. https://doi.org/10.1039/c1gc15349h.

(8) Ferrari, A. C.; Robertson, J. Interpretation of Raman Spectra of Disordered and Amorphous Carbon. *Phys Rev B* **2000**, *61* (20), 14095–14107. https://doi.org/10.1103/PhysRevB.61.14095.

(9) Sadezky, A.; Muckenhuber, H.; Grothe, H.; Niessner, R.; Pöschl, U. Raman Microspectroscopy of Soot and Related Carbonaceous Materials: Spectral Analysis and Structural Information. *Carbon N Y* **2005**, *43* (8), 1731–1742. https://doi.org/10.1016/j.carbon.2005.02.018.

(10) Ortlieb, N.; Martin, J.; Guggolz, L.; Ihonen, J.; Fischer, A. ^{13} C-Labeled Mesoporous N-Doped Carbon Nanospheres and N-Doped Hydrothermal Carbon Aerogels as Model Materials for Carbon Corrosion Determination in Electrode Structures. *Adv Energy Mater* **2025**. https://doi.org/10.1002/aenm.202406164.

(11) Maass, S.; Finsterwalder, F.; Frank, G.; Hartmann, R.; Merten, C. Carbon Support Oxidation in PEM Fuel Cell Cathodes. *J Power Sources* **2008**, *176* (2), 444–451. https://doi.org/10.1016/J.JPOWSOUR.2007.08.053.

(12) Yu, X.; Ye, S. Recent Advances in Activity and Durability Enhancement of Pt/C Catalytic Cathode in PEMFC: Part II: Degradation Mechanism and Durability Enhancement of Carbon Supported Platinum Catalyst. *J Power Sources* **2007**, *172* (1), 145–154. https://doi.org/10.1016/J.JPOWSOUR.2007.07.048.

(13) Chen, H.; Zhao, X.; Zhang, T.; Pei, P. The Reactant Starvation of the Proton Exchange Membrane Fuel Cells for Vehicular Applications: A Review. *Energy Convers Manag* **2019**, *182*, 282–298. https://doi.org/10.1016/J.ENCONMAN.2018.12.049.

7. APPENDIX

7.1 Appendix A.

Properties of Vulcan XC72R

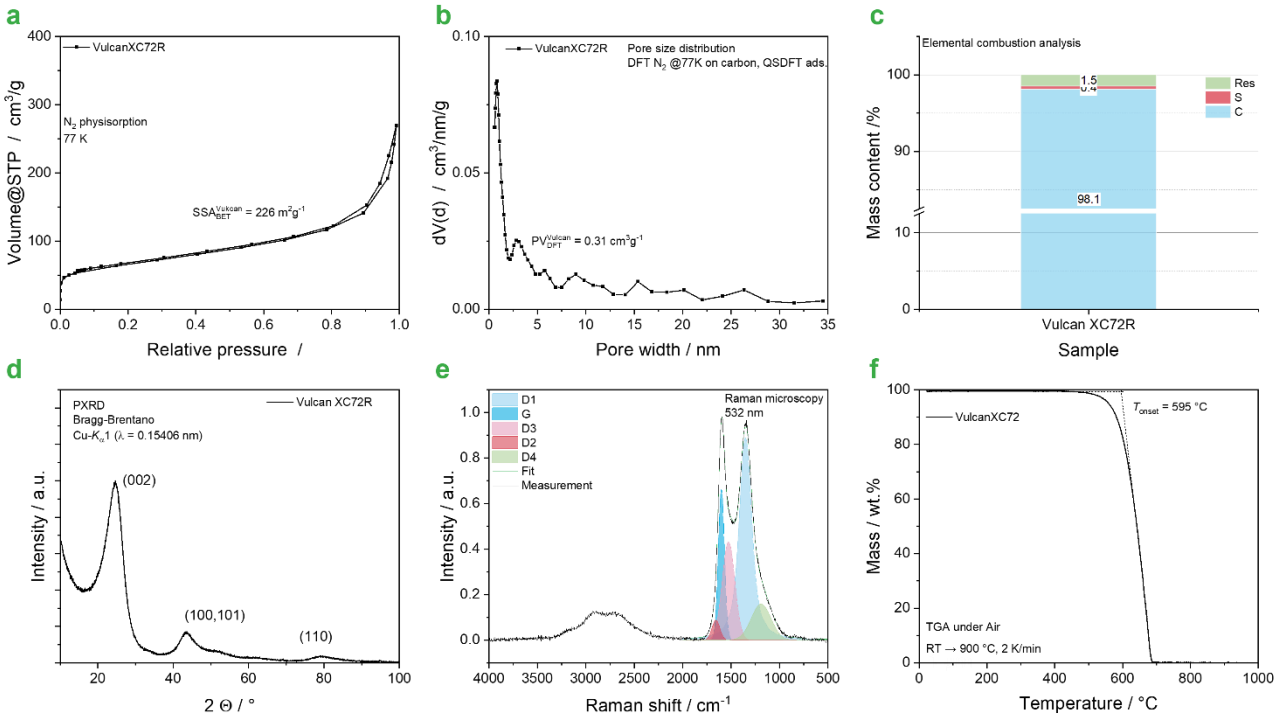

Figure 13: Vulcan XC72R characterization. *a) Nitrogen physisorption isotherm and b) Pore size distribution (DFT model). c) Elemental combustion analysis. d) Powder X-Ray diffraction. E) Raman microscopy. f) TGA measurement under air.*

Properties of first attempts of N-HTC large-scale synthesis: Non-optimized large-scale N-HTC characterization

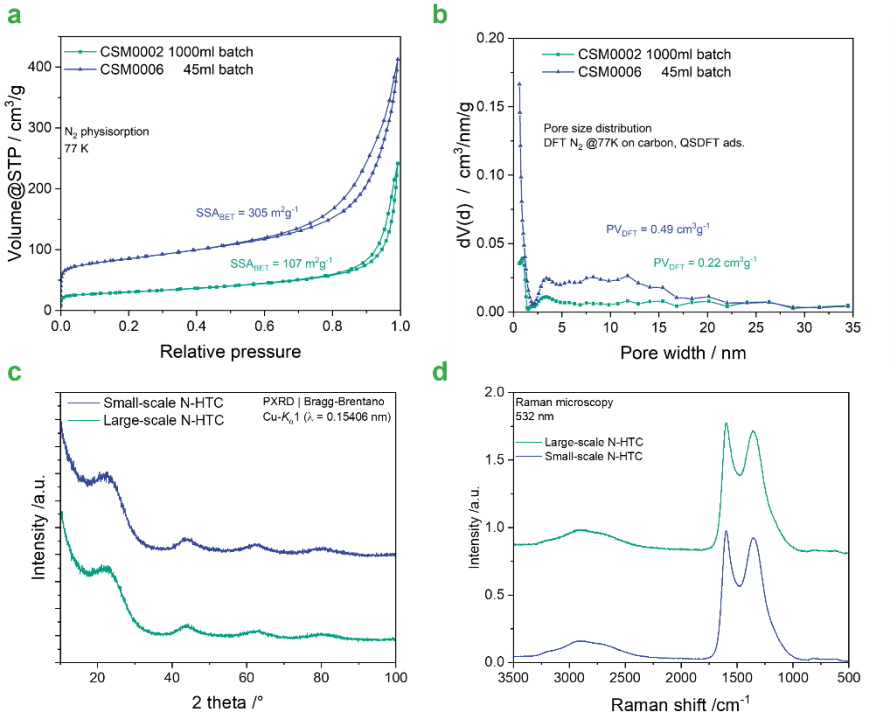

Figure 14: Non-optimized large-scale N-HTC characterization. *a) Nitrogen physisorption isotherm and b) Pore size distribution (DFT model). c) Elemental combustion analysis. d) Powder X-Ray diffraction. E) Raman microscopy. f) TGA measurement under air.*